

# DextrES: Wearable Haptic Feedback for Grasping in VR via a Thin Form-Factor Electrostatic Brake

Ronan Hinchet<sup>1,†</sup>, Velko Vechev<sup>2,‡</sup>, Herbert Shea<sup>1</sup>, Otmar Hilliges<sup>2</sup>

<sup>1</sup>EPFL, <sup>2</sup>ETH Zurich

{ronan.hinchet, herbert.shea}@epfl.ch, {velko.vechev, otmar.hilliges}@inf.ethz.ch

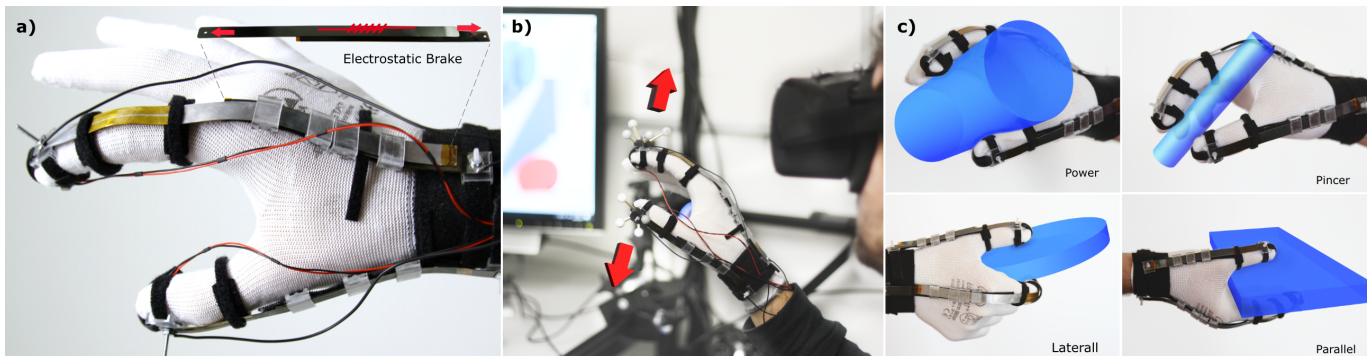


Figure 1. DextrES is a flexible and thin form-factor haptic feedback mechanism for precise manipulation of virtual objects in VR and AR. a) Our approach provides kinesthetic feedback via electrostatic brakes and piezoelectric actuators for cutaneous feedback. b) We experimentally show that DextrES improves precision of virtual object manipulations in VR across c) a number of different types of grasps, each affording different hand poses.

## ABSTRACT

We introduce DextrES, a flexible and wearable haptic glove which integrates both kinesthetic and cutaneous feedback in a thin and light form factor (weight is less than 8g). Our approach is based on an electrostatic clutch generating up to 20 N of holding force on each finger by modulating the electrostatic attraction between flexible elastic metal strips to generate an electrically-controlled friction force. We harness the resulting braking force to rapidly render on-demand kinesthetic feedback. The electrostatic brake is mounted onto the the index finger and thumb via modular 3D printed articulated guides which allow the metal strips to glide smoothly. Cutaneous feedback is provided via piezo actuators at the fingertips. We demonstrate that our approach can provide rich haptic feedback under dexterous articulation of the user’s hands and provides effective haptic feedback across a variety of different grasps. A controlled experiment indicates that DextrES improves the grasping precision for different types of virtual objects. Finally, we report on results of a psychophysical study which identifies discrimination thresholds for different levels of holding force.

<sup>†</sup>Authors contributed equally to this work.

Permission to make digital or hard copies of all or part of this work for personal or classroom use is granted without fee provided that copies are not made or distributed for profit or commercial advantage and that copies bear this notice and the full citation on the first page. Copyrights for components of this work owned by others than the author(s) must be honored. Abstracting with credit is permitted. To copy otherwise, to republish, to post on servers or to redistribute to lists, requires prior specific permission and/or a fee. Request permissions from [permissions@acm.org](mailto:permissions@acm.org).

UIST '18, October 14–17, 2018, Berlin, Germany

© 2018 Copyright held by the owner/author(s). Publication rights licensed to ACM. ISBN 978-1-4503-5948-1/18/10...\$15.00

DOI: <https://doi.org/10.1145/3242587.3242657>

## Author Keywords

Haptics; VR; electrostatic brake; dexterous interaction

## INTRODUCTION

The dexterity of the human hand enables us to perform a number of useful everyday tasks such as actively exploring surfaces and grasping and moving objects [20, 16]. In Virtual Reality (VR), dexterous manipulation using the hand is a popular means of interaction. It allows us to leverage learned motor skills and vice versa, to train for real-world scenarios in VR [19]. While rapid progress has been made on the input side (display and sensing technologies), haptic interfaces providing physical feedback to the hand lag behind in their fidelity. In particular, the lack of appropriate kinesthetic feedback limit our ability to precisely steer and place grasped objects in 3D space [34].

The ability to grasp objects is amongst the most useful skills we can perform in VR [8]. One challenging aspect is the wide array of possible grasps which require the fingers to be free to move into different configurations [16]. Traditionally, grasping feedback in VR has been supported via glove-based exoskeletons which create braking forces on the fingers [12, 21], render localized tactile feedback on the fingertips [13, 31], or combine aspects of both [10, 22]. These devices often employ complex mechanisms placed around the hand which may either add weight, constrain the movement of the fingers, or both. As a result, the full range of interaction capabilities of the human hand are under-utilized.

To address this challenge, we introduce DextrES, a finger-mounted haptic mechanism capable of achieving up to 20N of holding force on each finger when flexing inward. Our

novel approach is based on electrostatic attraction to create a rapidly controlled braking force between two electrically charged strips of metal. We harness the resulting braking force to rapidly render on-demand kinesthetic feedback which blocks the motion of the fingers. Crucially, this allows for the design of a very thin and flexible form factor haptic interface for grasping objects in VR - a long standing goal which has thus far relied on space-inefficient and bulky mechanisms. Such an interface may also be generalized to function beyond VR, for example in Augmented Reality (AR), robotic tele-operation, and rehabilitation applications.

In contrast to a one-size-fits-all mounting solution, we integrate DextrES onto the index finger and thumb using modular fittings with different strip lengths inserted into 3D printed articulated guides to keep them moving smoothly. The strips are anchored onto the fingertip and wrist resulting in controlled frictional forces due to sliding when the finger is flexed. This mounting strategy allows for easy adaptation to different hand sizes. We couple our kinesthetic brake with miniature vibration motors mounted at each fingertip to signal initial contact events, mimicking a typical object manipulation cycle [24]. The resulting integration into VR allows freedom of movement for both the fingers and hand. The volume of the control electronics can be reduced to a few  $cm^3$  with off-the shelf components, and the very low power consumption (less than 100 mW) allows for battery powered operation, providing a straightforward path to widespread real-world implementation.

We test the capabilities of DextrES in two experiments. First, we establish the just noticeable difference (JND) at different voltage levels and associate this to equivalent holding forces and perceived stiffness values. Second, we explore the impact of our feedback mechanism on the precision of four different grasps (see Figure 1c) in a VR environment. Results indicate that DextrES provides effective feedback and improves precision. Finally, we report qualitative results and user feedback on the perceived user experience when interacting in a free-form VR environment.

## RELATED WORK

### *Haptic Components of Grasping*

The perceptual mechanisms behind the experience of holding an object or exploring the shape and texture of its surface is composed of *kinesthetic* and *cutaneous* components [23]. Kinesthetic feedback is based on larger scale forces while cutaneous stimuli are felt by the pressure receptors in the skin, typically in the fingertips. During object manipulation, the typical cycle starts when type 1 fast receptors in the fingertips are excited for about 1 second, indicating the contact boundary of an object [24]. After initial contact, kinesthetic forces are transmitted through the joints and muscles, informing us of relative limb and finger positions through the sense of proprioception. Kinesthetic and cutaneous channels work in tandem to provide an accurate sensation of touch [43] that also acts as a feedback loop to accurately control the grasping force exerted on an object [47].

### *Grasping in Virtual Reality*

Researchers have replicated various types of forces in VR which are rendered when grasping an object, including gravity [7, 30], contact [31], shearing [42], rendering hard surfaces [21], and spring-back [8]. While many different types of grasps are possible [16], most grasping devices focus on finger-opposition power grasps. Grounded devices can create high fidelity feedback [29, 1], but are fixed in position. Hand-held VR controllers such as the Oculus Rift and HTC Vive allow the user to move his or her arms freely, but occupy the grasp thus prevent most hand movements, as well as only render coarse vibro-tactile feedback. Our approach consists of a thin form-factor electrostatic brake which can render kinesthetic and cutaneous haptic feedback in a wide range of grasps, affording a rich set of interactive capabilities.

### *Kinesthetic haptic feedback gloves*

Haptic feedback gloves have a long history in HCI and VR research [35]. A number of exoskeletal devices have been proposed to provide kinesthetic haptic feedback by blocking fingers' movement. We can distinguish between gloves based on pneumatic or hydraulic systems, and those based on electromechanical systems. Gloves based on fluids generally use pumps and valves [22] to displace pistons [17, 5] or activate jamming layers [49, 6] on the glove. These technologies are well-known, but difficult to miniaturize and can result in complex and bulky systems. Gloves using magnetorheological fluids have also been reported [4, 48]. Gloves using electromechanical principles mostly make use of motors or brakes directly on the glove (early versions used very long cables [12]). They use servo motors linked to bars/rods over the top of the hand [28, 27] or cables (tendon-based) across the top of the hand [12, 10, 44] to control finger position. They can actively steer mechanical linkages for finer control. Others have used motors to drive clamp braking mechanisms in order to block the finger [8, 21].

Motors or pumps can offer significant forces, but their performance decreases quickly when scaled down. It is very difficult to maintain sufficient force if scaled to volumes of a few cubic centimeters. Larger motors or pumps may be acceptable for VR but it would be disturbing for AR [35]. It would be ideal to directly be able to lock the finger position without using motors, just by blocking or clutching directly jointless flexible links (cables or strips) connected to the finger. We report here such a solid-state device, a jointless exoskeleton where the only moving parts are actuated by the user.

### *Electrostatic braking mechanisms*

Numerous types of brakes, and more generally clutches, have been developed. Electromagnetic clutches are the most common type of electrically driven clutch, but are bulky and have high power consumption [38]. Mechanical latches can significantly decrease power consumption at the cost of increased complexity and reduced speed. Magnetorheological (MR fluid) clutches are simpler but heavier and consume more energy [46, 40, 45]. Such clutches or brakes are not well suited to haptic gloves for VR and AR applications, where the wearable haptic systems should be as comfortable and discreet as possible.

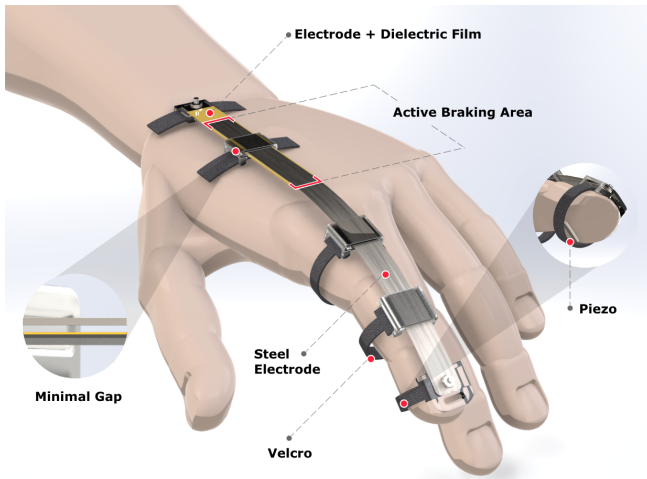


Figure 2. Schematic representation of the components of our haptic feedback mechanism. ES brakes along the fingers provide kinesthetic feedback and piezo actuators provide cutaneous feedback. The total weight is less than 8 grams. The ES brake is flexible, allowing for natural hand motion and hence a variety of grasps.

Early development of electrostatic (ES) clutches started in 1923 [25] and brakes have been used since 1957 [18]. Similar principles were used for lateral sliding ES actuators [32, 33]. ES clutches have been developed more recently for applications in robotics [14, 2, 26, 39]. ES clutches are an interesting alternative to electromagnetic clutches at mm scale [14]. Their design is compact and simple, they can be low profile, flexible, and lightweight. Furthermore, they can generate high forces with ms time. Once the electrodes are charged, power consumption becomes extremely low. In light of these advantages, we leverage ES clutches as the core element of thin-form factor electrically driven haptic gloves able to provide kinesthetic haptic feedback.

## SYSTEM OVERVIEW

The aim of our work is to provide haptic feedback for dexterous manipulation of virtual objects in VR and AR. The ideal feedback mechanism would be able to provide both *kinesthetic* and *cutaneous* feedback [23] while not encumbering the natural motion of the users fingers and requiring minimal user instrumentation. This is challenging to achieve since most mechanisms that can provide sufficient force to block finger motion also require significant user instrumentation and are bulky.

Recent work has therefore opted to only support haptic feedback for a limited number of hand poses via actuation mechanisms that are build into a VR controller [3, 9].

In contrast, our work explores the use of an ES brake as thin-form factor kinesthetic feedback mechanism that can be integrated into a VR glove without hindering the natural motion of the fingers. Together with piezo actuators, mounted at the fingertips, DextrES, illustrated in Figure 2, provides both kinesthetic and cutaneous feedback and can thus support a variety of grasps and enables precise VR manipulations.

## Challenges

While the basic concept of ES brakes is straightforward and has been leveraged for non-haptic applications, designing an effective feedback mechanism for VR is not. To allow for unencumbered motion, the device needs to be thin-form factor and lightweight. Yet to provide effective haptic sensations, it must produce sufficient forces and must be easily mounted on users' hands of varying sizes. Throughout this paper we discuss our solutions to the following challenges:

**(1) Fabricating an ES Brake.** The brake must have sufficient force, speed, be robust, have a low-form factor and sub-Watt power consumption. These requirements impact material and thickness choices for the conductor and insulator layers. Since the brake must conform to the finger shape, the metal strips must be made from a strong and flexible material able to repeatedly bend, yet also provide a small restoring force, thus excluding ductile metals like copper or soft materials like conductive fabrics. The dielectric layer also impacts mechanical and electrostatic aspects and must hence be chosen to be thin enough to attain useful forces without requiring tens of kV, must have a high breakdown field and very low leakage current. Furthermore the dielectric must be flexible and smooth enough to allow accurate control of frictional forces to allow or block the sliding of the strips.

**(2) Haptic Glove Integration** The human hand moves in complex ways, typically modeled by a total of 27 degrees-of-freedom [15]. This dexterity poses significant challenges for the design of haptic feedback mechanisms. First, the braking mechanism must be securely mounted onto the users' hand such that it can effectively brake the motion of fingers in arbitrary poses. To effectively deal with metacarpal abduction (particularly challenging for the thumb) the force needs to be anchored at the back of the hand. Furthermore, to allow for natural motion the brake should not create friction when disengaged. Finally, to accommodate varying hand sizes the mounting mechanism must be flexible and modular.

**(3) VR Integration.** Since VR affords a very immediate form of interaction, a haptic feedback mechanism should be able to function efficiently under arbitrary hand poses. In particular, humans use a variety of grasps [16] and as many as possible of these should be supported. To support dexterous object manipulation in VR, the braking mechanism must be able to engage and dis-engage almost instantaneously to allow for rapid, natural hand motion corresponding to a realistic sensation of grasping and releasing virtual objects.

## ELECTROSTATIC BRAKING MECHANISM

In this section we present the working principle, fabrication process and performance of the electrostatic kinesthetic haptic feedback brakes.

### Operation principle

At the heart of our approach is a laminar electrostatic (ES) brake. Our ES brake consists of 18 cm long thin flexible metal strips that slide freely when no control voltage is applied, but generate up to 20 N of holding force per pair of strips when a suitable control voltage is applied. One of the key features of the ES brake is its thin form-factor, ideal for

wearable applications. The active part of the brake is conformable to fingers and can be directly mounted or inserted on a glove. The brake mass on the glove is 8 g, and it is 6 mm high (including attachments).

As shown in Figure 1, the ES brake is attached to the glove, covering the back of the hand and the back of the finger. The high degree of flexibility allows excellent conformity to any hand shape. Figure 3 shows the structure of a single ES brake strip (the strips can be stacked to increase force). Each brake element consist of two 100  $\mu\text{m}$  micron thick steel strips, separated by a thin insulation layer bonded to one strip, thus forming a variable capacitor  $C_{strip}$ :

$$C_{strip} = \frac{\epsilon_r \epsilon_0 A}{d}, \quad (1)$$

where  $\epsilon_r$  is the relative permittivity of the insulator between the electrodes,  $\epsilon_0$  is the permittivity of vacuum,  $A$  is the overlap area between the electrodes, and  $d$  is the thin dielectric gap between the electrodes. One strip (the “hand strip”) is attached via the glove to a fixed point on the back of the hand, while the other strip (the “finger strip”) is attached via the glove to a fingertip. When the voltage difference between the strips is zero, the strips freely slide with a very low friction, enabling full and unimpeded finger movements (Figure 3b). In the simplest model of the device, when a voltage  $V$  is applied between the strips, an attractive electrostatic force  $F_{compression}$  is generated between the strips, pulling them together (Figure 3c) :

$$F_{compression} = \frac{\epsilon_r \epsilon_0 A V^2}{2d^2}, \quad (2)$$

This electrically-controlled normal force leads to frictional forces between the strips, partially or fully blocking the movement of the finger. The friction force is less than or equal to the friction coefficient  $\mu$  times  $F_{compression}$ :

$$F_{friction} \leq \mu F_{compression}. \quad (3)$$

The higher the applied voltage, the higher the friction force. Using this ES brake, we can thus apply a high blocking force to the fingers, providing kinesthetic haptic feedback.

The power consumption  $P_{ESbrake}$  of the brake is determined by the energy to charge the capacitor multiplied by the switching frequency  $f$ :

$$P_{ESbrake} = \frac{E}{t} = \frac{1}{2} C V^2 f \quad (4)$$

Operating at 20Hz and 1.5 kV, the device power consumption is less than 60 mW.

### Fabrication of the ES brake

After introducing the general working principle we now detail our solutions to challenge Nr. 1 as outlined in the System Overview Section.

We chose stainless steel as conductor since it is a reliable spring material. The bending stiffness of a strip scales approximately with the cube of the shim thickness. One must find a suitable compromise between being thick enough for

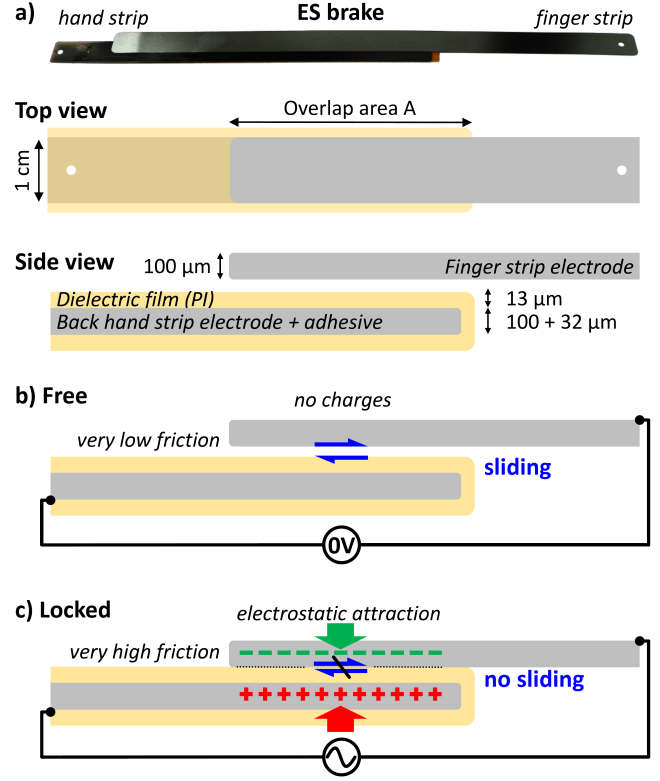


Figure 3. Schematic of the ES brake. a) Picture of the ES brake’s hand strip and finger strip. Top view of the 1 cm wide hand strip and finger strip overlapping one another. Side view of the strips describing the materials and thickness of each layers. b) Free sliding between the strips when the voltage difference is 0 V. c) When a voltage is applied between strips, the electrostatic attraction pulls the strips together, drastically increasing the sliding friction.

the shim to slide easily without buckling or plastically deforming, yet thin enough so that the force to bend the strip is nearly imperceptible.

The fabrication of the ES brake strips consists of 3 steps: first, two strips 18 cm long and 1 cm wide were laser cut from 100  $\mu\text{m}$  thick stainless steel sheets. Strips are shortened at a later time to fit the user’s hand and fingers. Second, after polishing the edges, we deposited by hand onto the top surface of the “hand strip” a 32  $\mu\text{m}$  thick conductive double-side adhesive and a 13  $\mu\text{m}$  thin polyimide film, slightly wider than the steel shim to avoid short circuits. Polyimide has a high breakdown field of over 300 V/ $\mu\text{m}$  and a dielectric constant of 3.4. Using a conductive adhesive to attach the polyimide to the steel was a key step in reducing the driving voltage, as the adhesive is thus part of the electrode rather than being part of the dielectric. The fabrication process is straightforward, low-cost and readily industrialized.

### Control Electronics for ES brake

To actuate and control the ES brake, we assembled a custom high voltage (HV) power source [37], based on a 2000 V DC-DC converter (XP Power, EMCO) with a maximum output power of 1 W and a maximum current of 500  $\mu\text{A}$  for safety. It is coupled with an H-bridge using opto couplers (MPI Technologies) to generate a square-wave AC signal at



**Figure 4.** Assembly of the ES brake, 3D printed guides and attachments fastened to thin nylon glove using velcro.

a frequency of up to 1 kHz. The HVS was controlled by an Arduino micro controller via a USB connection to a laptop. For a fully portable application, the electronics can be scaled down to a few  $cm^3$ . The use of HV in wearable devices is not a problem as long as the current is very small. Hence, we limited the current to  $500 \mu A$ . In addition, strips and connections can easily be enameled or insulated. In our case, the users' hand was insulated using a nylon glove and Polyimide tape.

We used bipolar square waves at 10 or 20 Hz. AC operation eliminates charge injection in the dielectric layers, a problem we had observed after continuous DC actuation. AC actuation thus allows the electrostatic force to be turned off as soon as the voltage is reduced, even after hours of continuous operation. It comes at the cost of marginally higher power consumption (tens of mW).

### HAPTIC GLOVE INTEGRATION

The ES braking mechanism needs to be integrated into a glove form-factor so as to effectively provide haptic feedback (Challenge Nr. 2). We explored multiple configurations for clutch placement (e.g., finger vs. back of the hand), attachment means to finger tip, wrist, or forearm, investigated different positions to account for the multiple degrees of freedom of the thumb, etc. We report here only the configuration that gave the best results.

### Glove assembly

We mount the ES brakes on a glove covering the index finger and the thumb via velcro fabric hook and loop fasteners, 3D printed wrist and finger tip anchors (4.5 mm high and 16 mm wide) and 3D printed guides (6 mm high and 14 mm wide), see Figure 4. Assembly is straightforward and can account for variations of hand size, geometry (static) and flexibility (dynamic) across users. To deliver effective haptic feedback, the ES Brake must conform as much as possible to the hand and be firmly attached to it.

### Finger flexion and abduction

The fingers consist of 3 phalanges (2 for the thumb), with joints able to bend up to 90 degrees and with radius of curvature of just a few  $mm$ . This range of motion can cause problems when bending a stack of sliding strips. We therefore designed the "hand strip" to be slightly shorter than the "finger strip". The "finger strip" is attached to the finger tip and covers the phalanges and the metacarpus while the "hand strip" is attached to the wrist and only covers the carpus and metacarpus. The overlap region covers the metacarpus on the back of the hand, anchoring the force so that it can counteract finger flexion.

Another challenge arises from the metacarpo-phalangeal (MCP) joint which can both flex and abduct. If not counteracted, under abduction the free end of the "finger strip" will laterally slide on the back of the hand while rotating the finger, causing misaligned strips and reduced braking force. It is important to maintain a constant distance between the strips, even under deformation. Finally, a misaligned strip can damage the insulating layer. To avoid this, we polished the strips' edges and covered the strips' free ends with insulating tape. We use 3D printed guides to keep the strips aligned on the back of the hand, requiring the "finger strip" to be flexible enough to accommodate finger rotation.

### Thumb

The thumb is composed of only two phalanges and a flexible metacarpus. Designing an ES Brake for the thumb proved to be more difficult than for other fingers. The ES Brake device is the same for all fingers (only its length changes) but its integration on the glove is different for the thumb. We empirically found that to be effective and to support the Power, Pincer, Lateral and Parallel grasps (Figure 1c) we had to tilt the thumb strips anchors 30 degree outward. Moreover, the hand strip had to be attached further back on the wrist compared to the index finger (Figure 1a).

### Glove activation and deactivation

In the simplest model, the electrostatic force scales as  $1/gap^2$ , thus having a small initial distance between strips is critical. We carefully designed our 3D printed guides to ensure that a) the strips are as close together as possible, and b) leave just enough room for smooth gliding to allow fast retraction. To activate the brakes, each ES strip is set to 1 kV at 20 Hz. Once a small region of the strip pairs come into contact, the adhesion propagates in a zipper-like effect. To deactivate the brakes, the difference of electrical potential between the strips is set back to 0 V.

### INTEGRATION INTO VR

#### Tracking and Haptic Device Control

Creating a convincing method of grasping objects in VR requires precise tracking of the fingers in order to determine when contact has been made. For tracking, we use an OptiTrack tracking system with 10 Prime 13 W cameras running at 240 Hz and custom designed rigid bodies that screw into the tips of the fingers. The centroids of the rigid bodies are calibrated to sit in the center of the finger such that finger collisions in real life match finger collisions in VR. The mean

tracking error after calibration of the whole system was  $< 1$  mm. An Oculus CV1 headset is used to display the virtual scene. The coordinate systems are aligned via a calibration procedure built into the Motive:Tracker software. We use Unity to render the VR scenes. The position of the fingers are displayed as small spheres. Each haptic controller (index, thumb, piezo) has a separate physical connection (USB) and are controlled individually over different serial ports.

#### Grasping Method

We implement a custom grasping algorithm, similar to Choi et al. [9] using a kinematic approach. A grasp begins when the position of each finger (index, thumb) are within 5 mm of a virtual object and the object to be grasped is between the fingers. Once the object is grasped, the resulting ray between the two fingers is used to kinematically rotate and re-position the object in real time, and to calculate the amount of object penetration for analysis. The grasp ends when the ray between the fingers exceeds its original starting (euclidean) distance. This approach ensures a steady and natural feeling grasp and supports more types of grasps than off-the-shelf solutions such as the Leap Motion Interaction Engine.

#### Haptic Rendering

When a user grasps an object, we activate index and thumb brakes simultaneously. Any slack will initially be perceived as zero blocking force, but as soon as the slack is taken up, it will be perceived as a sudden locking of the finger. Mechanically, the strips counteract torque in the DIP and hence directly brake the downward motion of the fingertip. The perceived effect is that of grasping an object in real life, despite not directly generating a normal force. It is possible that a user could squeeze hard enough to break the adhesion, however, this would exceed normal grip forces during grasps which are shown to be two times the load force [47].

In accordance with perceptual theory on initial contact during object manipulation [24], the feeling of grasping can be improved by adding tactile feedback at the fingertips. For this task, we use tiny vibration motors (PiezoVibe from Murata) which measure  $3.8 \times 10.5 \times 2$  mm and vibrate at 240 Hz. They generate an acceleration of 1.2 G for a mass of 20 g and consume 6 mW. When a grasp begins, we briefly activate the piezos for 0.3s to indicate the start of a touch event. They are not re-activated during release.

#### SYSTEM EVALUATION

Before reporting on our usability experiments we briefly characterize the ES brakes in terms of blocking force vs. applied voltage and for response speed.

#### ES Brake predicted force and speed

Based on Equation 2 and Equation 3, and considering an ES brake having an overlap of  $A=11 \text{ cm}^2$ , a  $13 \text{ }\mu\text{m}$  Polyimide insulator film with relative dielectric constant 3.4 and a friction coefficient of 0.2 between kapton and steel [41], a voltage of 1500 V should generate a compression force of 220 N, resulting in a friction force of 44 N. Using our HV supply with a maximum current of  $500 \text{ }\mu\text{A}$ , it should take 50 ms to fully charge the strips, thus enabling up to 20 Hz operation. At this frequency, the ES brake consumes 57 mW (Equation 4).

#### Measurement method

To measure the braking force of our ES brake, we placed it in a pull tester (Instron 3344L) equipped with a 50 N load cell (Instron 2519). This allows us to pull on the ES brake over 10 mm while measuring the braking force (Figure 5a).

#### Experimental results

Figure 5b plots the braking force generated by the ES brake vs. time for a pull speed of 1 mm/s for a 10 Hz AC actuation voltages ranging from 0 V to 1500 V (Figure 5b). The force starts at zero and quickly increases as any slack is taken up. The force then reaches a plateau corresponding to the braking force. At maximum load, we noted repeated slipping and slip-stick behavior as a result of the AC actuation.

Results are summarized in (Figure 5c) for 16 measurements on several devices. Our ES brakes can block up to 20 N at 1500 V and 10 Hz with variations of 10 %. This corresponds to a force of  $2 \text{ N/cm}^2$ . It is possible to stack ES brakes to achieve higher forces or to reduce the operating voltage at constant force. When switching between 0 V (free) and 1500 V (locked), we observed a response time of less than 100 ms. This correspond to a force slew rate higher than 200 N/s.

#### USER EVALUATION

To better understand the efficacy of DextrES and its possible applications, we conduct a quantitative and a qualitative experiment. First, a psychophysical evaluation measures the *just noticeable difference* (JND) of stiffness which can be felt on each finger. Second, we explore the grasping precision afforded by DextrES and its effect on the immersion of the user. Each study has been designed to answer the following research questions respectively:

- **RQ1:** What is the *just noticeable difference* of blocking force at different voltages at each finger (index, thumb) and what is their associated perceived stiffness?
- **RQ2:** What effect do the kinesthetic, cutaneous, and combined modes of DextrES have on the *precision* and *immersion* while grasping and manipulating objects in VR?

#### Study 1: Force Discrimination

While grasping devices have been created that can exert up to 100N of force per finger [8], it is not clear that such high forces are actually needed for dexterous manipulation of objects in VR. In this study, we are interested in the perceived stiffness rendered on each finger (thumb, index) and its JND. In order to create the feeling of different levels of perceived stiffnesses, we vary a reference input voltage, and use an adaptive staircase method [11] to determine the JND at each reference voltage. Based on pilot studies, we select three reference voltages (200 V, 400 V, 800 V) and a variable step size with an initial value of  $\Delta V$  to 7.5 %. Before the study, we measured the force output of the strips at each of the reference voltages and noted this for later analysis (see Fig. 5).

#### Participants

We recruited six healthy adult unpaid participants ( $M=30.8$ ;  $SD=3.1$ ; 1 female) from the ETHZ university campus. Participants had an average hand span of 21.7 cm ( $SD=1.5$ )

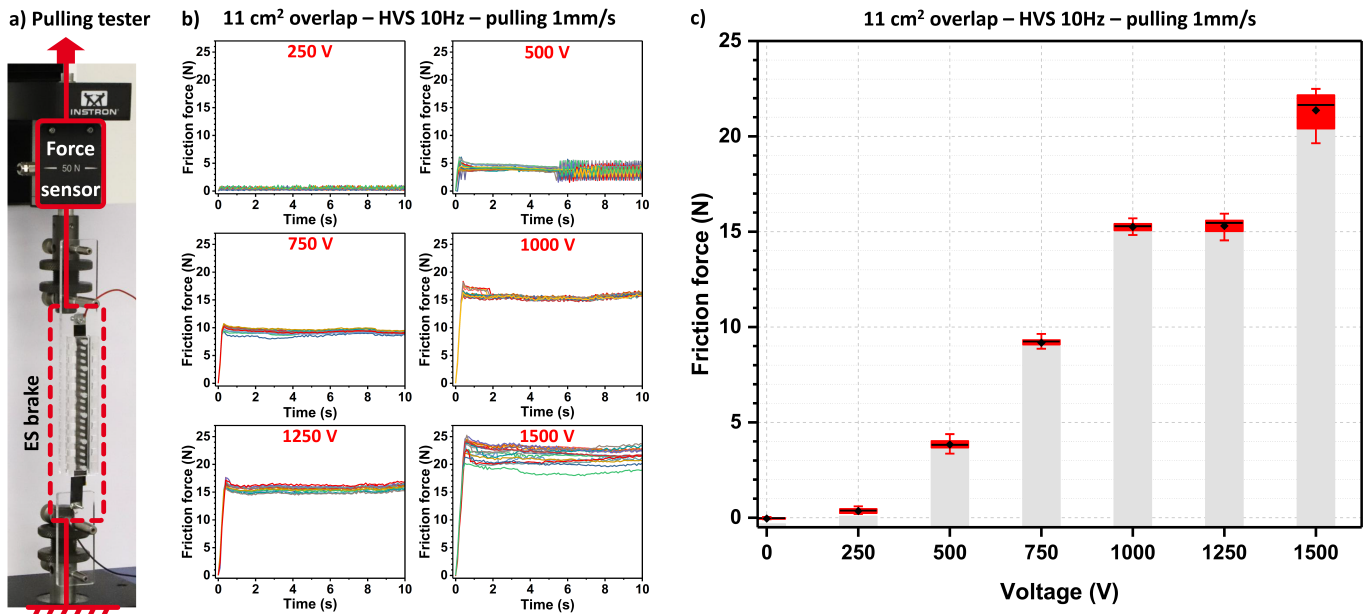


**Figure 5.** Friction force measurements. a) Pull tester setup to measure the ES brake’s friction force. b) Measured braking force for voltages from 250 V to 1500 V vs time as the strips are pulled apart at 1 mm/s. The initial overlap area was 11 cm<sup>2</sup>. The frequency of the AC actuation was 10 Hz. c) Friction force vs. applied voltage. The black dot is the average, the black line is the median, the box correspond to the IRQ and the bars to the min-max. Higher is better.

as measured from the end of the pinky finger to the thumb. Each participant signed an informed consent form prior to the study.

#### Procedure and Task

The braking mechanism was mounted on the index finger and thumb of each participant. Since we only test one finger at a time, the mounting of the 3D printed guides and their velcro holders can be placed in straight lines extending from the tip of both the index finger and thumb, with the thumb configured in the abducted position. Participants are then given some practice time to get accustomed to the device, after which they put on noise-canceling headphones and a blindfold in order to eliminate interference from external visual and auditory senses. The JND for each finger is then determined using the adaptive staircase procedure [11] described above.

Each trial consists of two runs with randomized presentation order. In one run, the fixed reference voltage is activated, and in the other run, the approaching voltage is activated. On each run, the participant flexes their finger inwards until they sense the blocking force. The participant is unaware of which voltage is used. The initial value for the approaching voltage is +25 % of the reference value. In the case of 800 V, it was set at -25 % of the reference voltage, however positive and negative JND approaches are typically symmetric [19]. After each trial, we ask participants to identify which of the two voltages was perceived to be blocking their finger more. A correct response brings the voltage in the next trial a step size towards the reference voltage, and vice versa [11]. The step size was halved to 3.75 % after the first direction reversal in order to get more accuracy after the initial approach. The procedure is repeated until the direction is reversed 3 times and the reversal points are averaged to get the JND of each

starting condition. At the end of the procedure, participants answered how stiff they perceived the blocking force to be.

#### Results

Table 1 summarizes the JND for each finger in different positions and reference voltages. The smallest JND for both fingers is in the middle range (400 V), where participants could adequately sense about 5% differences in blocking force.

Based on the perceived stiffness at this voltage, it is possible for DextrES to render objects with different levels of deformable stiffness. At the low end (200 V), the JND rises significantly as we approach a perceptibility threshold. At the high end (800 V), participants were considerably more perceptible than expected and perceived stiffness is still not close to maximum, meaning there is still some room to render objects with very hard but still deformable stiffnesses if the voltage is increased even further. Comparing between the middle and high reference, the results are non-linear, which suggests that there is an upper bound on rendering an object of maximum stiffness.

#### Study 2: Grasping Precision and Realism in VR

To answer RQ2, we conduct a VR study measuring both quantitative aspects of precision during object manipulation, and qualitative aspects of realism during the grasping of objects. We use the same definition of grasp as Feix et al. [16] where grasping stipulates that objects are held firmly in the hand (rigid) and not rotated by moving the fingers (static).

#### Participants

Ten healthy adult subjects ( $M=27.6$ ;  $SD=4.14$ ; 2 female) were recruited for our study. Two participants had no previous experience with VR and 1 participant was left-handed.

Location	JND			Blocking Force (Measured)			Perceived Stiffness		
	200V	400V	800V	200V	400V	800V	200V	400V	800V
Index Finger	20.6 %	5.6 %	7.8 %	0.10 N	1.34 N	6.04 N	1.2	2.3	3.8
Thumb	15.2 %	4.6 %	10.1 %	0.16 N	1.05 N	3.91 N	1.5	1.8	4.2

**Table 1. JND Study results at three different reference voltages. Blocking force equivalent was pre-measured for each set of strip combinations. Perceived stiffness is rated on a 5-points Likert scale where 1 is easily deformable and 5 is a rigid object that cannot be deformed.**

Each participant signed an informed consent form prior to the study.

#### Procedure

The procedure is described to the participant alongside a brief introduction to the device and its function. The ES brake strips are then mounted to the back of the hand and adjusted as described earlier. Participants could sit in a 1x1 meter tracking area wearing an Oculus headset. Participants wore noise-canceling headphones to remove external audio cues when grasping objects. The experiment consisted of two scenarios, the first evaluating the quantitative aspect measuring grasping precision, the second, qualitative aspects comparing the realism of grasping objects between different haptic feedback conditions. The experiment took 1.5 hours to complete.

Participants could practice freely in order to learn four different grasps (*Lateral, Parallel, Pincer, Power* see Figure 1) and to get used to the different types of feedback. After training, 4 blocks were completed of 16 unique grasp/condition combinations for 64 trials in total. The quantitative part was followed by approximately 1 min of each condition in a physics playground which was designed to resemble a typical desk with various sized items which could be grasped and interacted with. The experiment concluded by participants indicating their subjective preferences and a short interview on the overall impression of the experience in using DextrES. We also recorded suggestions for possible applications of our device and informal comments.

#### Design

For the quantitative study, a within-subject design was used with two independent variables: *Grasp* {*Lateral, Parallel, Pincer, Power*} and *Feedback* {*Visual, Piezo, Brake, Both*}. The order of each stimuli was randomized such that each combination of *Grasp* and *Feedback* was presented once per block. As dependent variables, we measured *time* and *precision* for each trial. Precision was measured by the percentage of finger-object penetration averaged over the whole trial.

At the end of the physics playground scenario, we asked participants to rate how realistic the sensation of holding an object is in each feedback condition on a 7-point Likert-scale (1: Extremely unrealistic, 7: Extremely realistic). We also ask about the comfort of the device while turned off (1: Very uncomfortable, 7: Very comfortable) and the freedom of movement (1: Fully blocking, 7: Full range of motion).

#### Task, Stimuli and Apparatus

Trials were initialized and terminated via pressing a virtual button, or after a 20 second timeout. Each *Grasp* has an associated task (see Fig. 6 for visuals and explanation) which is derived from real-life tasks. Participants were instructed

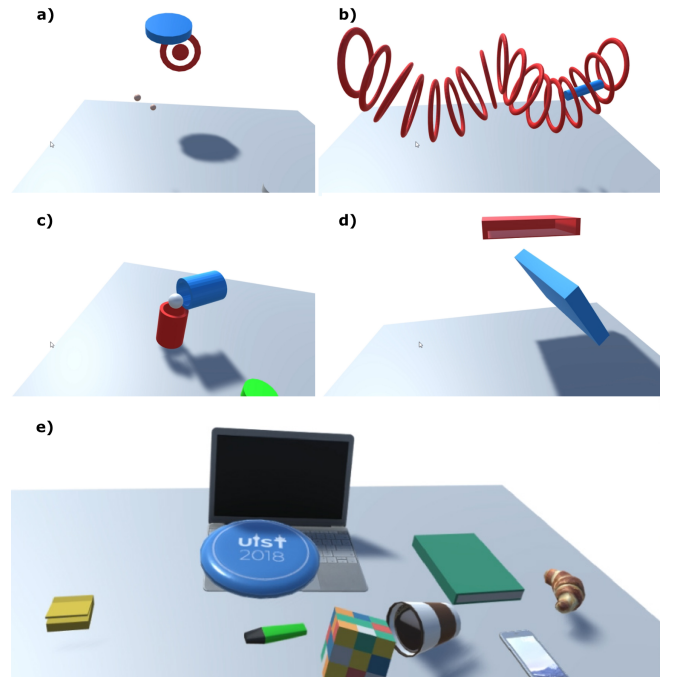


**Figure 6. Experiment tasks. Manipulated objects in red, target in blue: a) hitting target with frisbee (*lateral grasp*). b) Steering task (*pincer*). c) Ball-in-cup (*power*). d) Bookshelf (*parallel*). e) Physics playground.**

to complete the task in timely manner as accurately as possible. The instructions given in regards to grasping an object were to perform it as naturally as possible. After each block participants could take a break before proceeding.

#### Quantitative Results

To assess the effect of the different feedback mechanisms on grasp precision we ran a repeated measures ANOVA for each grasp. There was no difference in terms of task completion times. Since the four grasps are significantly different it does not make sense to compare feedback mechanisms across the four grasps. We now report main effects and pairwise post-hoc comparisons for all four grasps (*lateral, parallel, pincer, power*) respectively. The sphericity assumption was not violated for any of the grasps. All *p*-values of pairwise comparisons are Bonferroni corrected.

For the *lateral* condition (e.g., turning a key) a main effect for the feedback mechanism ( $F_{3,27} = 5.17, p < 0.01$ ) was detected. A post-hoc analysis reveals that *both* is significantly more precise than *brake* ( $p = 0.02$ ) but differences to other conditions are not statistically significant.

The *parallel* grasp (e.g., lifting a book) yields similar results. The analysis again shows a main effect ( $F_{3,27} = 4.86, p <$

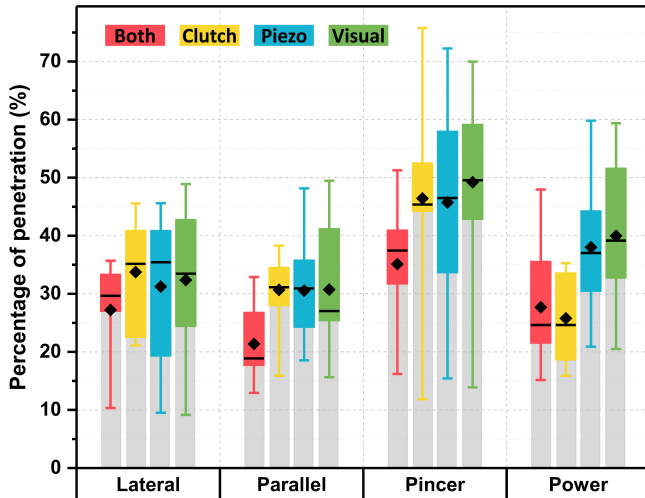


Figure 7. Effect of feedback mechanism on precision of 4 grasp types. Conditions are *both* (red), *brake* (blue), *piezo* (yellow) and *visual* (green). The black dot is the average, the black line is the median, the box correspond to the IRQ and the bars to the min-max. Lower is better.

0.01) and post-hoc analysis reveals that there is a significant difference between *both* and *brake* ( $p = 0.04$ ), albeit inspecting the plot in (Figure 7) shows that the differences are very small and this result should be interpreted carefully.

The remaining two grasps show a more marked effect of the feedback mechanism on the precision of the grasp, perhaps because both *pincer* and *power* admit much more finger motion (cf. Discussion section). There is a main effect for *pincer* ( $F_{3,27} = 12.24, p < 0.01$ ) and pairwise comparisons indicate that *both* is significantly more precise than *brake* ( $p = 0.01$ ), *piezo* ( $p = 0.02$ ), and *visual* ( $p < 0.01$ ). Finally, the *power* grasp also yields a main effect ( $F_{3,27} = 21.32, p < 0.01$ ). The pairwise comparisons indicate that for this grasp *brake* is the most precise. However, compared with *both* ( $p > 0.05$ ) the difference is not statistically significant. Both (*brake*, *both*) feedback mechanisms are however statistically more significant than the (*piezo*, *visual*) baselines (*both* vs *piezo*: ( $p = 0.01$ ), *both* vs *visual*: ( $p < 0.01$ )).

## Qualitative Results

### Subjective Rankings

The physics playground gave participants a chance to interact freely with virtual objects. In terms of the realism (see Figure 8) of the sensation of holding an object participants consistently rated the *both* feedback condition the highest ( $M=5.3$ ;  $SD=0.5$ ), followed by the *brake* ( $M=4.4$ ;  $SD=0.8$ ) and *piezo* ( $M=3.5$ ;  $SD=1.1$ ), and finally the *visual* only feedback ( $M=2.2$ ;  $SD=0.8$ ). Participants rated the device as mounted on the hand as fairly comfortable ( $M=5.1$ ;  $SD=1.4$ ), and the freedom of movement as neutral in terms of limiting finger motion ( $M=4.6$ ;  $SD=0.8$ ).

### Participant Comments

Participants strongly favored the combined feedback, which produced the highest sense of VR immersion (e.g., “Haptic is missing from VR, and I’m really impressed that it can block.” and “It’s pretty cool. It adds a lot of immersion.”),

and also helped to identify when grasping an object begins “It helped me understand when I should stop applying force”. The brake-only condition was slightly less preferred due to missing collision information “When you go and touch something you expect your skin to be bump into it”. When the brake was missing, participants could sense its absence “As soon as you go to the next trial and it’s off, then you miss the feedback”. Two participants preferred the piezo over the brake on its own, however, it was still rated as less realistic as just the brake (e.g. “Its very useful to know when you touch it, but its not a realistic feeling”). Furthermore, the brake adds

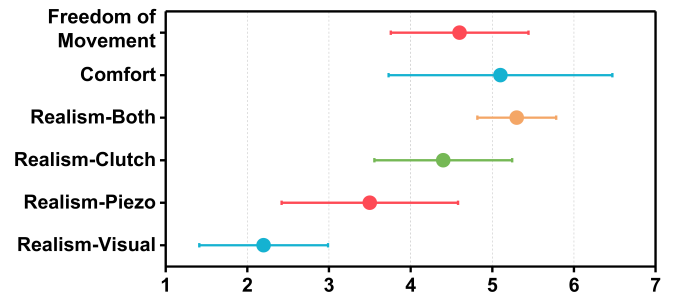


Figure 8. Subjective feedback on 7-point Likert scale. Dot is the mean and bars indicate confidence interval. Higher is better.

realism in the context of limiting range of motion (e.g. “If you hold a bigger object, then if you rotate you should have more limited range of motion”) (because the forearm muscles engage). Some participants found DextrES to provide physical support, specifically in the lateral grasp “When I got tired, I was using the brake to rest my thumb”). The main issue w.r.t. to comfort was the feeling of velcro on the hand, but on the whole, participants felt that DextrES was comfortable to wear. In terms of applications, participants wanted to use the device to play games, for virtual typing, and also for creative tools such as CAD tools and painting (e.g. “You can 3D paint, but maybe different sized brushes have different weight”).

## DISCUSSION

A major contribution of our work is to **fabricate an ES brake** for VR. Through careful material selection, specifically the use of a conductive adhesive to minimize effective dielectric thickness and a dielectric with high breakdown fields, in combination with a flexible mechanical design that allows for dimension tailoring and achieves reliable sliding over curled fingers, and by using AC switching of the 1.5 kV power supply to avoid charge injection, we were able to develop an ES brake with suitable force generation capabilities while allowing natural hand motion. Including mounting hardware, DextrES weighs under 8 g, yet can block 20 N when on, with only a few mN of residual force when off. We thus have a blocking force density over 2500 N/kg, while delivering a device so flexible it is barely perceivable on the hand. The materials are all readily commercially available, and can be machined in minutes with a laser cutter.

The ES brake was **integrated into a glove** using close-fitting 3D printed attachments on the fingertips and wrist, by precise positioning of 3D printed guides on the glove, by aligning the index brake with the index’s long extensor tendon, and by placing most of the active part of the brake on the back of the

hand where there is much less deformation. The thumb was most challenging, principally due to its more complex motion (not only can it flex like the fingers, but it can also pivot on 2 axis), making it harder to mount the ES brake in a way that effectively blocks flexion. There is also little room on the back of the hand to mount the brake and a medium curvature close to the wrist attachment. We found that aligning the thumb ES Brake 30 degrees outward of the thumb flexion axis gave the most blocking. While more direct forms of tactile feedback are available [36, 3], integrating such devices in their current form may interfere with the mounting of the strips and the natural motion of the hand.

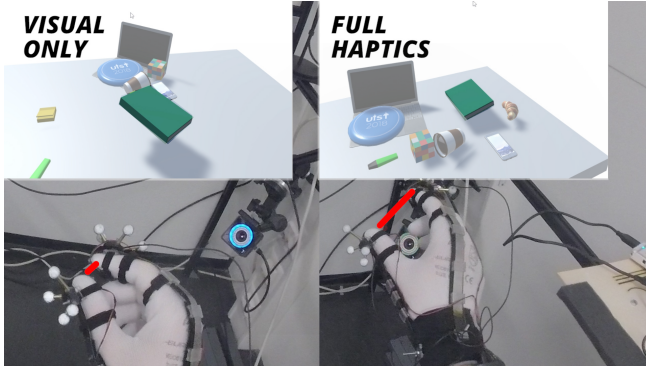


**Figure 9.** Examples of differences in grasps across conditions. Left: without haptic feedback, participants penetrate virtual objects. Right: with haptic feedback, fingers conform to the object’s shape (green book).

The final challenge of **VR integration** was also met. The results from our VR grasping study indicate that DextrES is able to support three of the four grasps (Parallel, Pincer, Power), in particular when both the brake and piezo work in tandem. Participants were able to both pick up and drop objects in a natural fashion and experience a sensation of holding an object. The main differentiating factor between grasps is the distance between the tip of the index finger and the thumb. In the Power grasp, this distance is wide, and thus gives some space for the brake to engage and to exhaust any mechanical slack. As a result, the *brake* and *both* conditions perform similarly. In the Pincer and Parallel grasps, this distance is small, thus they greatly benefit from the additional collision signal from the Piezo. With regards to the Lateral grasp, this distance is also small. Furthermore, the inward flexion of the thumb does not necessarily induce any sliding motion on the strips of the brake, and thus neither the piezo or the brake have much stopping effect. While the brake cannot constrain certain degrees of freedom of the thumb in the Lateral grasp, participants enjoyed that they could rest their thumb after the brake has engaged.

The above results show that DextrES is able to increase precision during specific VR manipulations. In some cases and for some participants the differences were small in the controlled experiment. However, in the more natural setting of the physics playground, participants exhibited very different behavior. They were less careful when picking up and handling objects and thus tended to penetrate through them completely in the visual and piezo conditions (see Figure 9, left), whereas with haptic feedback they conformed to the object’s

shape (see Figure 9, right). In part, this explains the large differences in the perceived realism in holding an object compared to the smaller differences we see when looking at the percentage of penetration in the controlled experiment. While we do not directly test grasping objects of variable stiffness in VR, results from the force discrimination study suggests that this is a possibility.

## CONCLUSIONS AND FUTURE WORK

We have presented DextrES, a novel haptic glove integrating electrostatic braking using flexible components. With its low mass (under 8 g) and high force (over 20 N) it overcomes limitations of more traditional motors and pumps. Our experimental results indicate that DextrES is a very promising step towards soft, flexible, high-speed wearable haptics conveying the sense of grasping with high realism. We tested the device for 4 grasps and found improved grasping precision for different virtual objects. By including small piezoactuators at the fingertips, we further increased the grasping precision.

Naturally, there is much room for future work. We plan to reduce the operating voltage by an order of magnitude by printing thinner dielectric layers or layers with higher permittivity. Lower voltage operation will: i) make the control electronics more compact and much cheaper since all components can be sourced in surface mount format (SMD), ii) reassure users who may be concerned about high voltages, iii) ease regulatory processes for wearables. Users currently are aware of the 20Hz switching, which can be distracting. Lower voltage operation would allow the device to be run with a sine wave rather than a square wave, greatly reducing the audible vibration. Further, the force generation capabilities may be increased by stacking several ES brakes.

In terms of haptics, it will be interesting to produce a five-fingered version of DextrES and to study it in more fully fledged VR and AR scenarios, and to explore the interplay between cutaneous and kinesthetic feedback in different manipulation tasks. To free up the fingertips in AR, the piezos could be moved to the side of the fingers and contact forces transmitted through the vibration of curved metal plates.

Finally, we note that it may be possible to reconstruct the hand pose via measuring the change in capacitance of the overlapping metal strips in combination with an inverse kinematics model of the human hand, removing the need for external tracking.

As wearables and VR become more mainstream, richer unobtrusive wearable haptic feedback becomes increasingly important. Lightweight and very low-profile gloves such as DextrES will allow users to benefit from rich and high-force haptics without excessive user instrumentation.

## ACKNOWLEDGEMENTS

This work was supported in part by a grant from the Hasler Foundation (Switzerland). We thank Simon Perrault for his help in the statistical analysis, Sahar Ayvaz for his contribution in the mechanical design, Alexandru Dancu for experiment design feedback, Lilia Leung for illustration work,

Nadine Besse for mounting the piezo-actuators, Sam Schlatter for electronics advice, Juan Zarate for helpful discussions, and all participants for taking part in our experiments.

## REFERENCES

1. Araujo, B. et al. Snake Charmer: Physically Enabling Virtual Objects. In *Proceedings of the TEI '16: Tenth International Conference on Tangible, Embedded, and Embodied Interaction*, TEI '16, ACM, 2016, 218–226.
2. Aukes, D. M. et al. Design and testing of a selectively compliant underactuated hand. *The International Journal of Robotics Research* 33, 5 (apr 2014), 721–735.
3. Benko, H. et al. NormalTouch and TextureTouch: High-fidelity 3D Haptic Shape Rendering on Handheld Virtual Reality Controllers. In *Proceedings of the 29th Annual Symposium on User Interface Software and Technology*, UIST '16, ACM, 2016, 717–728.
4. Blake, J., and H. B. Gurocak. Haptic glove with mr brakes for virtual reality. *IEEE/ASME Transactions On Mechatronics* 14, 5 (2009), 606–615.
5. Bouzit, M. et al. The Rutgers Master II-new design force-feedback glove. *IEEE/ASME Transactions on Mechatronics* 7, 2 (jun 2002), 256–263.
6. Choi, I. et al. A Soft, Controllable, High Force Density Linear Brake Utilizing Layer Jamming. *IEEE Robotics and Automation Letters* 3, 1 (jan 2018), 450–457.
7. Choi, I. et al. Grability: A wearable haptic interface for simulating weight and grasping in virtual reality. In *Proceedings of the 30th Annual ACM Symposium on User Interface Software and Technology*, ACM, 2017, 119–130.
8. Choi, I. et al. Wolverine: A wearable haptic interface for grasping in virtual reality. In *Intelligent Robots and Systems (IROS), 2016 IEEE/RSJ International Conference on*, IEEE, 2016, 986–993.
9. Choi, I. et al. Claw: A multifunctional handheld haptic controller for grasping, touching, and triggering in virtual reality. In *Proceedings of the 2018 CHI Conference on Human Factors in Computing Systems*, ACM, 2018, 654.
10. ContactCI. Maestro Glove. <http://www.contactci.com>. Last accessed: 03.05.2018.
11. Cornsweet, T. N. The staircase-method in psychophysics. *The American journal of psychology* 75, 3 (1962), 485–491.
12. CyberGlove Systems Inc. CyberGrasp Glove. <http://www.cyberglovesystems.com/cybergasp>. Last accessed: 12.03.2017.
13. CyberGlove Systems Inc. CyberTouch Glove. <http://www.cyberglovesystems.com/cybertouch>. Last accessed: 18.03.2017.
14. Diller, S., C. Majidi, and S. H. Collins. A lightweight, low-power electroadhesive clutch and spring for exoskeleton actuation. In *2016 IEEE International Conference on Robotics and Automation (ICRA)*, IEEE, may 2016, 682–689.
15. ElKoura, G., and K. Singh. Handrix: animating the human hand. In *Proceedings of the 2003 ACM SIGGRAPH/Eurographics symposium on Computer animation*, Eurographics Association, 2003, 110–119.
16. Feix, T. et al. The grasp taxonomy of human grasp types. *IEEE Transactions on Human-Machine Systems* 46, 1 (2016), 66–77.
17. Festo. HexoHand Glove. <https://www.festo.com/group/en/cms/10233.htm>. Last accessed: 04.04.2018.
18. Fitch, C. J. Development of the Electrostatic Clutch. *IBM Journal of Research and Development* 1, 1 (jan 1957), 49–56.
19. Fu, W., M. M. van Paassen, and M. Mulder. The influence of discrimination strategy on the jnd in human haptic perception of manipulator stiffness. In *AIAA Modeling and Simulation Technologies Conference*, 2017, 3668.
20. Gibson, J. J. Observations on active touch. *Psychological review* 69, 6 (1962), 477.
21. Gu, X. et al. Dexmo: An inexpensive and lightweight mechanical exoskeleton for motion capture and force feedback in vr. In *Proceedings of the 2016 CHI Conference on Human Factors in Computing Systems*, ACM, 2016, 1991–1995.
22. HaptX. HaptX Glove. <https://www.haptx.com>. Last accessed: 03.05.2018.
23. Hayward, V. et al. Haptic interfaces and devices. *Sensor Review* 24, 1 (2004), 16–29.
24. Johansson, R. S., and J. R. Flanagan. Coding and use of tactile signals from the fingertips in object manipulation tasks. *Nature Reviews Neuroscience* 10, 5 (2009), 345.
25. Johnsen, A., and K. Rahbek. A physical phenomenon and its applications to telegraphy, telephony, etc. *Journal of the Institution of Electrical Engineers* 61, 320 (jul 1923), 713–725.
26. Karagozler, M. E. et al. Electrostatic latching for inter-module adhesion, power transfer, and communication in modular robots. In *2007 IEEE/RSJ International Conference on Intelligent Robots and Systems*, IEEE, oct 2007, 2779–2786.
27. Kim, H., M. Kim, and W. Lee. HapThimble: A Wearable Haptic Device Towards Usable Virtual Touch Screen. In *Proceedings of the 2016 CHI Conference on Human Factors in Computing Systems*, CHI '16, ACM, 2016, 3694–3705.

28. Lelieveld, M. J., T. Maeno, and T. Tomiyama. Design and development of two concepts for a 4 dof portable haptic interface with active and passive multi-point force feedback for the index finger. In *ASME 2006 International Design Engineering Technical Conferences and Computers and Information in Engineering Conference*, American Society of Mechanical Engineers, 2006, 547–556.
29. Massie, T. H., J. K. Salisbury, et al. The phantom haptic interface: A device for probing virtual objects. In *Proceedings of the ASME winter annual meeting, symposium on haptic interfaces for virtual environment and teleoperator systems*, vol. 55, Citeseer, 1994, 295–300.
30. Minamizawa, K. et al. Gravity grabber: wearable haptic display to present virtual mass sensation. In *ACM SIGGRAPH 2007 emerging technologies*, ACM, 2007, 8.
31. Moehring, M., and B. Froehlich. Effective manipulation of virtual objects within arm's reach. In *Virtual Reality Conference (VR), 2011 IEEE*, IEEE, 2011, 131–138.
32. Niino, T., S. Egawa, and T. Higuchi. High-power and high-efficiency electrostatic actuator. In *[1993] Proceedings IEEE Micro Electro Mechanical Systems*, IEEE, 1993, 236–241.
33. Niino, T. et al. Development of an electrostatic actuator exceeding 10 N propulsive force. In *[1992] Proceedings IEEE Micro Electro Mechanical Systems*, IEEE, 1992, 122–127.
34. Pacchierotti, C. et al. Two finger grasping simulation with cutaneous and kinesthetic force feedback. In *International Conference on Human Haptic Sensing and Touch Enabled Computer Applications*, Springer, 2012, 373–382.
35. Pacchierotti, C. et al. Wearable haptic systems for the fingertip and the hand: Taxonomy, review, and perspectives. *IEEE transactions on haptics* 10, 4 (2017), 580–600.
36. Pece, F. et al. Magtics: Flexible and thin form factor magnetic actuators for dynamic and wearable haptic feedback. In *Proceedings of the 30th Annual ACM Symposium on User Interface Software and Technology*, ACM, 2017, 143–154.
37. PetapicoVoltron. Peta-pico-Voltron Project. <http://petapicovoltron.com/>. Last accessed: 12.07.2018.
38. Plooij, M. et al. Lock Your Robot: A Review of Locking Devices in Robotics. *IEEE Robotics & Automation Magazine* 22, 1 (mar 2015), 106–117.
39. Prahlad, H. et al. Electroadhesive robotswall climbing robots enabled by a novel, robust, and electrically controllable adhesion technology. In *Robotics and Automation, 2008. ICRA 2008. IEEE International Conference on*, IEEE, 2008, 3028–3033.
40. Saito, T., and H. Ikeda. Development of Normally Closed Type of Magnetorheological Clutch and its Application to Safe Torque Control System of Human-Collaborative Robot. *Journal of Intelligent Material Systems and Structures* 18, 12 (dec 2007), 1181–1185.
41. Samyn, P. et al. Sliding properties of polyimide against various steel and DLC-coated counterfaces. In *Proceedings of of BALKANTRIB 05*, B. Ivkovic, Ed., 5th International Conference on Tribology, 2005, 506–515.
42. Schorr, S. B., and A. M. Okamura. Fingertip tactile devices for virtual object manipulation and exploration. In *Proceedings of the 2017 CHI Conference on Human Factors in Computing Systems*, ACM, 2017, 3115–3119.
43. Scilingo, E. P. et al. Rendering softness: Integration of kinesthetic and cutaneous information in a haptic device. *IEEE Transactions on Haptics*, 2 (2010), 109–118.
44. Sense Glove BV. Sense Glove. <https://www.senseglove.com>. Last accessed: 03.05.2018.
45. Shafer, A. S., and M. R. Kermani. Design and validation of a Magneto-Rheological clutch for practical control applications in human-friendly manipulation. In *2011 IEEE International Conference on Robotics and Automation*, IEEE, may 2011, 4266–4271.
46. Wang, D. M., Y. F. Hou, and Z. Z. Tian. A novel high-torque magnetorheological brake with a water cooling method for heat dissipation. *Smart Materials and Structures* 22, 2 (feb 2013), 025019.
47. White, O. et al. Do novel gravitational environments alter the grip-force/load-force coupling at the fingertips? *Experimental brain research* 163, 3 (2005), 324–334.
48. Winter, S. H., and M. Bouzit. Use of Magnetorheological Fluid in a Force Feedback Glove. *IEEE Transactions on Neural Systems and Rehabilitation Engineering* 15, 1 (mar 2007), 2–8.
49. Zubrycki, I., and G. Granosik. Novel haptic device using jamming principle for providing kinaesthetic feedback in glove-based control interface. *Journal of Intelligent & Robotic Systems* 85, 3-4 (2017), 413–429.